Engineering and Technology Journal e-ISSN: 2456-3358

Volume 11 Issue 05 May-2026, Page No.-9957-9963

DOI: 10.47191/etj/v11i05.30, I.F. – 8.595

A Study on Effects of Cutting Parameters on Surface Roughness in Dry Milling of Hastelloy C276

Nguyen The Doan

Department of Manufacturing Engineering, Faculty of Mechanical Engineering, Thai Nguyen University of Technology, Thai Nguyen, 250000, Vietnam

ABSTRACT: Hastelloy C276 is a nickel-based superalloy widely used in aerospace, chemical processing, and energy industries due to its excellent corrosion resistance and high mechanical strength. However, its low thermal conductivity and strong work-hardening behavior make the alloy difficult to machine, leading to poor surface quality. This study investigates the effects of cutting parameters on surface roughness (Ra) during dry milling of Hastelloy C276. Milling experiments were carried out on a Mazak Smart 530C vertical machining center using Titan-coated carbide inserts. A Box–Behnken response surface methodology was employed to design the experiments and analyze the influence of cutting speed (V), feed rate (f), and depth of cut (t) on machining performance. The developed regression models showed good agreement with the experimental data, with coefficients of determination of 93.86% for surface roughness. The results showed that feed rate was the most influential factor affecting surface roughness. Single-objective optimization determined the optimal set of parameters including V = 42 m/min, f = 0.08 mm/tooth and t = 0.2 mm for the minimum surface roughness value Ra = 0.1884 µm. The findings provide useful guidelines for improving machining performance of Hastelloy C276 in dry milling conditions.

KEYWORDS*:* Hastelloy C276; Dry milling; Cutting parameters; Surface roughness.

1. INTRODUCTION

Hastelloy is a nickel-based superalloy known for its high mechanical strength, excellent resistance to oxidation and corrosion, and the ability to maintain mechanical stability under extreme temperature and pressure conditions. These properties make it widely used in aerospace, chemical processing, nuclear, and power generation industries. The superior performance of Hastelloy mainly results from solid solution strengthening and precipitation mechanisms in the nickel matrix, which improve high-temperature strength and creep resistance. However, these characteristics also make Hastelloy difficult to machine compared with conventional engineering materials [1,2].

The machining of nickel-based superalloys has been extensively studied in manufacturing research. According to Taylor's classical metal cutting theory [3], machinability depends on cutting parameters, tool materials, and thermo-mechanical interactions at the tool–chip interface. Hastelloy typically exhibits low thermal conductivity and strong strain hardening behavior, which lead to high cutting temperatures, severe tool wear, and unstable chip formation, ultimately reducing tool life and machining efficiency [4,5].

Surface integrity is a critical factor when machining advanced alloys, including surface roughness, residual stress, microhardness, and microstructural changes induced during cutting. These characteristics significantly influence the functional performance and fatigue life of machined components. Previous studies have indicated that machining parameters strongly affect the formation of surface defects and subsurface damage in high-performance alloys [6–8].

Chip formation and cutting temperature are key aspects governing machining performance. Chip morphology is affected by cutting speed, feed rate, and tool geometry, while shear localization and segmented chip formation often occur in nickel-based superalloys due to their high strength and strain hardening properties [9,10]. Moreover, significant heat is generated in the shear zone and at the tool–chip interface, accelerating tool wear and degrading surface quality [11]. Therefore, predicting and controlling cutting temperature remains an important topic in machining research [12,13].

Recent studies have focused on improving machining performance through advanced tool materials, coatings, and modeling techniques. Hard coatings such as AlTiN and nanostructured coatings can improve tool wear resistance and thermal stability when machining difficult-to-cut materials [14,15]. In addition, analytical and numerical models have been developed to predict cutting forces, temperature distribution, and material behavior during machining processes [16,17].

This paper reviews the machining of Hastelloy alloys, focusing on chip formation, heat generation, tool wear, and surface integrity. It also discusses the influence of machining parameters, tool materials, and machining strategies on cutting temperature, surface quality, and tool life.

2. MATERIAL AND METHOD

The diagram of the experimental setup and measurements are shown in Figure 1. Milling experiments on the difficult-to-machine material Hastelloy C276 were performed on a Mazak smart 530C vertical milling machine (Japan). Titan coated carbide inserts designated S-APMT 1604 PDER Grade 8230S were mounted on a Ø25 face mill designated 25A6R024A25-SAD07D-C. The cutting force component values were measured using a Mitutoyo SJ-210 roughness gauge from Japan. In this study, the Hastelloy C276 workpiece dimensions were 23 × 60 × 40 mm. The chemical composition and mechanical properties of the Hastelloy C276 alloy steel are presented in Tables 1 and 2.

Figure 1. The set-up of milling experiment.

Table 1. Chemical composition of Hastelloy C276

Chemical composition (max %)								
Ni	Mo	Cr	Fe	W	Co	Mn	C	Si
56,47	15,02	15,86	6.59	3,66	1,22	0,96	0,01	0,03

Table 2. Mechanical properties of Hastelloy C276

Yield strength, MPa	Tensile strength, MPa	Elongation, %	Hardness range, HRC	Modulus of Elasticity (GPa)	Poison'Ratio n
355	760	40	30 - 32	200	0,32

3. RESULTS AND DISCUSSION

Box - Behnken response surface methodology was used to build an experimental design in order to study the influences of Cutting depth (*t*), cutting speed (*V*) and feed rate (*f*) on the Surface roughness *Ra (µm)* shown in Table 3. The chosen values of input variables were based on the previous work [18-20].

Table 3. Input variables and their levels

Input variables	**Symbol**	**Low level**	**High level**	**Responses**
Cutting depth (mm)	t	0.08	0.16	Surface Roughness *Ra (µm)*
Cutting speed (m/min)	*V*	30	70	
Feed rate (mm/tooth)	*f*	0.08	0.16	

The experiments were carried out by following the RunOrder. Each of the cutting trials was repeated three times under the same cutting condition and the average values of cutting force components were reported. The measured response results of the experimental design are summarized in Table 4.

Table 4. The experiment design with test run order and the measured Surface Roughness values

Std Order	**Run Order**	**PtType**	**Blocks**	**Input variables**			**Surface Roughness**
				t (mm)	***V* (m/min)**	***f* (mm/tooth)**	**Ra (µm)**
1	1	2	1	30	0.08	0.5	0.323
13	2	0	1	50	0.12	0.5	0.380

Std Order	**Run Order**	**PtType**	**Blocks**	**Input variables**			**Surface Roughness**
				t (mm)	***V* (m/min)**	***f* (mm/tooth)**	**Ra (µm)**
2	3	2	1	70	0.08	0.5	0.326
14	4	0	1	50	0.12	0.5	0.328
5	5	2	1	30	0.12	0.2	0.240
15	6	0	1	50	0.12	0.5	0.326
6	7	2	1	70	0.12	0.2	0.423
12	8	2	1	50	0.16	0.8	0.523
10	9	2	1	50	0.16	0.2	0.342
8	10	2	1	70	0.12	0.8	0.361
3	11	2	1	30	0.16	0.5	0.341
11	12	2	1	50	0.08	0.8	0.273
7	13	2	1	30	0.12	0.8	0.484
9	14	2	1	50	0.08	0.2	0.177
4	15	2	1	70	0.16	0.5	0.654

Minitab 21 software with significance level $\alpha = 0.05$ was used to analyze experimental data and obtain the results. The regression equation for the influences of investigated parameters on Surface Roughness *Ra* is given in equation 1 with the coefficient of determination $R^2 = 93.86\%$, which proves that the proposed model is consistent with the experimental data. The Pareto charts evaluate the effects of the investigated variables on Surface Roughness *Ra* given in Figures 2.

$$Ra(\mu m)=0.586-0.01724\,V-4.71\,f+0.891\,t+0.000143\,V*V+5.6\,f*f-0.277\,t*t+0.0972\,V*f-0.01273\,V*t+1.78\,f*t \quad (1)$$

In Figure 2, factors exceeding the reference line with a value of 2.57 are considered statistically significant and influence the surface roughness Ra. The most influential factors are the feed rate (f) to the depth of cut (t) and finally the cutting speed (V). The interaction effect between cutting speed and feed rate (V*f) and the interaction between cutting speed and depth of cut (V*t) also significantly influence the surface roughness Ra.

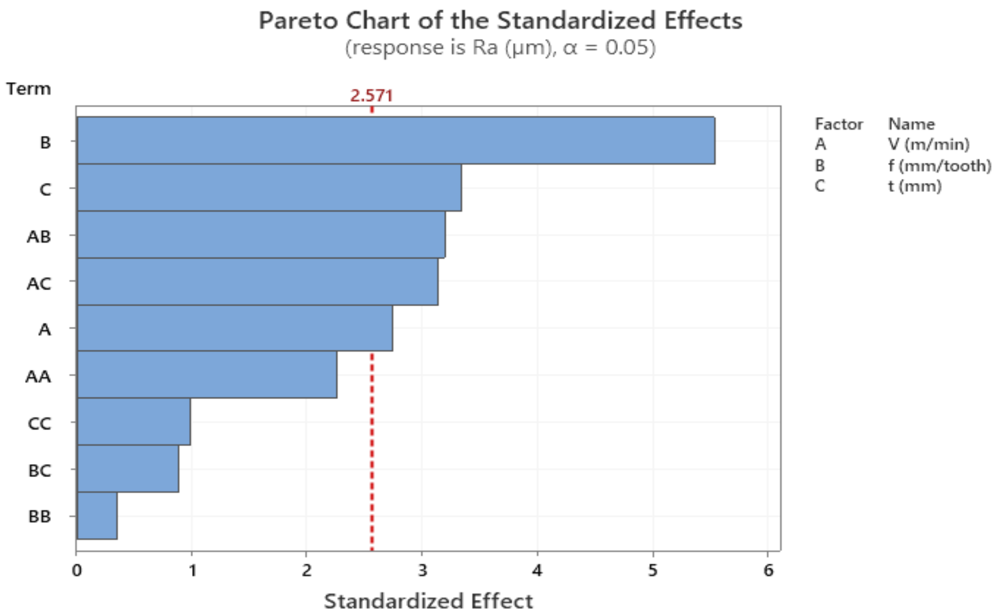

Figure 2. Pareto chart of influences of input variables on Surface Roughness Ra

From Figure 3, it can be observed that the surface roughness Ra varies noticeably with machining parameters during dry milling of Hastelloy C276. When the cutting speed increases from 30 m/min to around 40 m/min, the Ra value slightly decreases, indicating an improvement in the machined surface quality. This can be attributed to the reduction of material adhesion and built-up edge (BUE) formation at moderate cutting speeds, which stabilizes chip formation and improves the surface finish. However, when the cutting speed further increases to 70 m/min, the Ra value increases significantly. This may be caused by the higher cutting temperature, which accelerates tool wear and vibration during machining, thereby deteriorating the surface quality [21,22].

In addition, the surface roughness Ra increases continuously with the increase of feed rate from 0.08 mm/tooth to 0.16 mm/tooth. This is mainly because a higher feed rate increases the geometrical surface scallop height, while the higher cutting force intensifies plastic deformation and vibration in the cutting zone, leading to a rougher machined surface. Similar trends have been reported in the machining of nickel-based superalloys, where feed rate has a strong influence on surface roughness [23].

Meanwhile, Ra increases when the depth of cut rises from 0.2 mm to around 0.5 mm and then decreases when the depth of cut increases to 0.8 mm. The initial increase in surface roughness may be due to the rise in cutting force and vibration at larger depths of cut. However, when the depth of cut further increases, the cutting process becomes more stable and chip formation becomes more consistent, which can improve the surface quality. Furthermore, the high strength, strong work-hardening tendency, and low thermal conductivity of Hastelloy C276 significantly affect surface formation during machining [22,24].

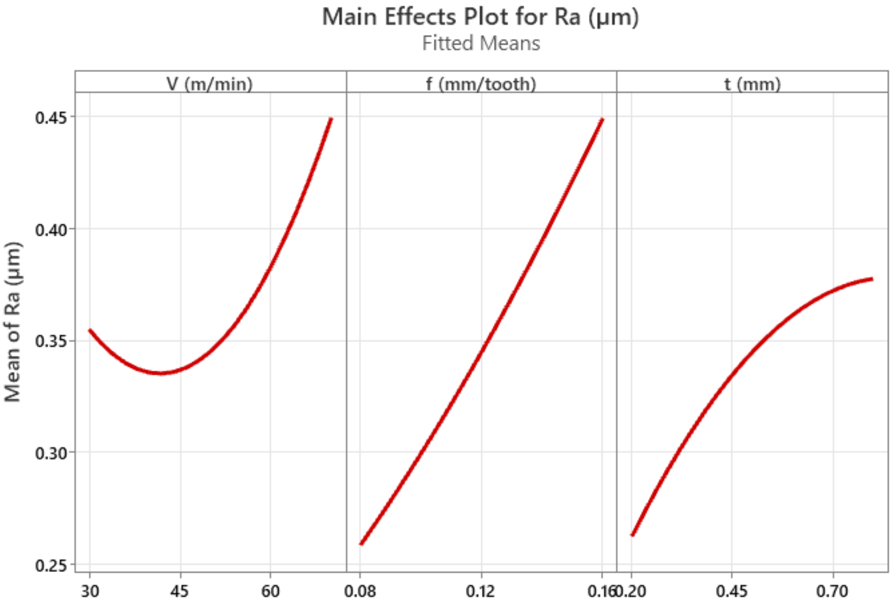

Figure 3. Main effects of investigated variables on the surface roughness Ra

The surface and contour plots of the influence of the studied variables on the surface roughness Ra are shown in Figures 4-6. In Figure 4, with f = 0.12 mm/tooth, it can be seen that a low depth of cut combined with a medium cutting speed will give the smallest cutting force coefficient (Figure 4a). Specifically, t = 0.2-0.22 mm and V = 30-32 m/min should be used to achieve a surface roughness Ra < 0.2µm (Figure 4b). In case t = 0.5 mm, the feed rate f = 0.08-0.10 mm/tooth and V = 38-70 m/min should be selected for surface roughness Ra < 0.2 µm (Figure 5). If V is kept constant at 50 m/min, the feed rate f = 0.08-0.085 mm/tooth and t = 0.2-0.25 mm should be selected to achieve the smallest surface roughness (Ra < 0.2 µm) (Figure 6).

Accordingly, V = 38-70 m/min, f = 0.08-0.085 mm/tooth and t = 0.2-0.25 mm would be reasonable ranges and can be selected to achieve smaller surface roughness.

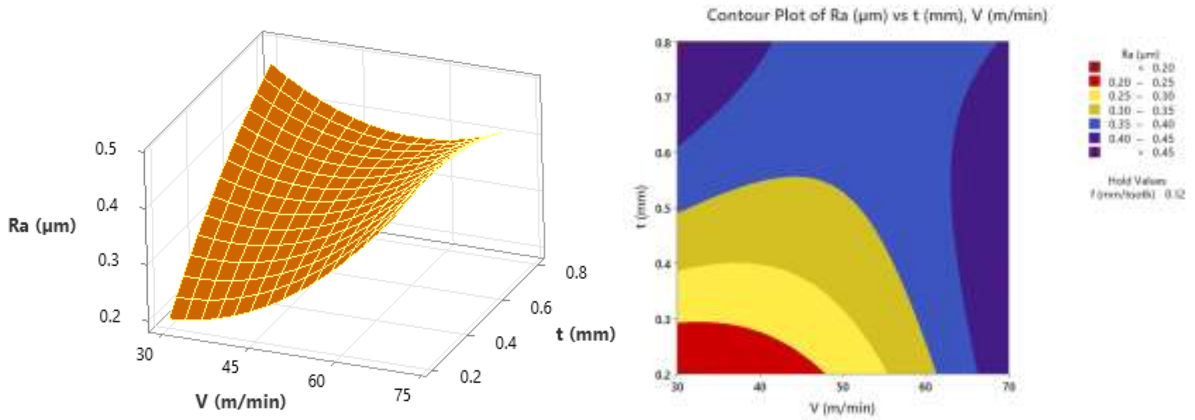

(a) Surface plot *(b) Contour plot*

Figure 4. Effects of cutting speed (V) and cutting depth (t) on the Surface Roughness Ra at a constant feed rate of f=0.12 mm/tooth.

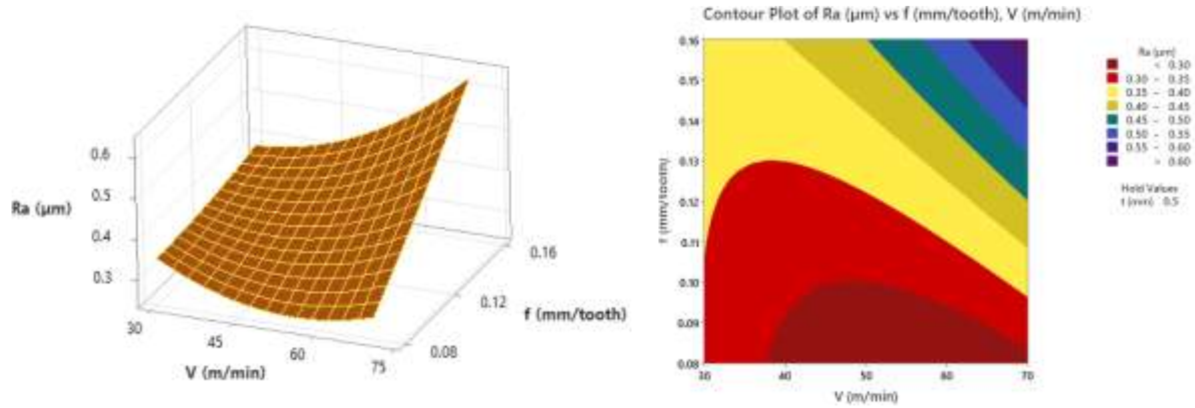

(a) Surface plot *(b) Contour plot*

Figure 5. Effects of cutting speed (V) and feed rate (f) on the Surface Roughness Ra at a constant cutting depth of t=0.5 mm.

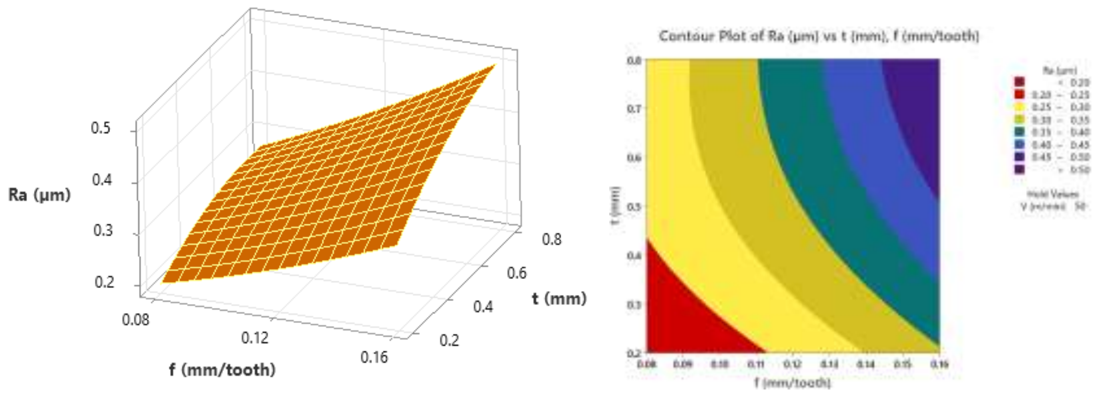

(a) Surface plot *(b) Contour plot*

Figure 6. Effects of cutting depth (t) and feed rate (f) on the Surface Roughness Ra at a constant cutting speed of V=50 m/min.

Through the obtained results shown in the surface and contour graphs, the selection process for the technological parameters will be quickly done to achieve the desired output values. However, to obtain the exact values, the optimization is needed. The optimization results for the surface roughness Ra are given in Figures 7. In Figure 7, the optimal value set V= 42.0443 m/min, f=0.08 mm/tooth and t=0.2 mm is determined to achieve the smallest surface roughness value R_a =0.1884 µm.

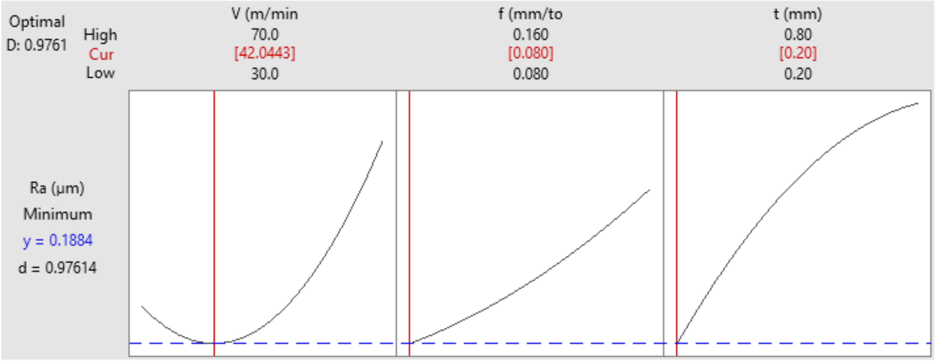

Figure 7. Optimization result for the surface roughness Ra

4. CONCLUSION

In this study, the influence of cutting parameters on machining performance in milling hastelloy C276 alloy steel was investigated. The influence of cutting speed, feed rate and depth of cut on surface roughness Ra was analyzed and evaluated. The main contributions of the study are summarized as follows:

Among the parameters surveyed, the feed rate has the greatest influence on surface roughness Ra. Besides that, cutting depth, cutting speed, the interaction between cutting speed and feed rate, and the interaction between cutting speed and cutting depth also affect Ra. Furthermore, surface roughness Ra can be used to evaluate the quality of the machined surface.

Reasonable technological guidelines for achieving smaller surface roughness Ra are provided. Specifically, V=38-70 m/min, f=0.08-0.085 mm/tooth and t= 0.2-0.25 mm should be proposed to achieve smaller surface roughness Ra.

Single-objective and multi-objective optimization were performed to determine the optimal set of values for the studied parameters. These optimal sets will provide valuable guidance for further research and practical applications.

In future studies, further investigations should focus on tool wear, tool life, and chip deformation mechanisms.

Acknowledgments: The study had the support of Thai Nguyen University of Technology, Thai Nguyen University, Vietnam.

Conflicts of Interest: The authors declare no conflict of interest.

REFERENCES

1. U. M. D. E. C. D. E. Los, ASM Metal Handbook, Volume 16: Machining, ASM International, 2005.
2. Grzesik W. Advanced machining processes of metallic materials. Elsevier; 2008.
3. F.W. Taylor, On the art of cutting metals, vol. 23. American society of mechanical engineers, 1906.
4. Woldman NE, Gibbons RC. Machinability and machining of metals. McGraw-Hill; 1951.
5. Zhirong Liao, Julius M. Schoop, Jannis Saelzer, Benjamin Bergmann, Yusuf Kaynak; Review of current best-practices in machinability evaluation and understanding for improving machining performance; CIRP Journal of Manufacturing Science and Technology 50 (2024) 151–184
6. Field M, Kahles JF, Cammett JT. A review of measuring methods for surface integrity. C I R P 1972;vol. 21(2):219–38.
7. Liao Z, et al. Surface integrity in metal machining-Part I: Fundamentals of surface characteristics and formation mechanisms. Int J Mach Tools Manuf 2021:103687.
8. la Monaca A, et al. Surface integrity in metal machining-Part II: Functional performance. Int J Mach Tools Manuf 2021:103718.
9. Nakayama K, Ogawa M. Basic Rules on the Form of Chip in Metal Cutting. in Gen Assem of CIRP, 28th, Manuf Technol 1978;vol. 27(1):17–21.
10. Komanduri R, Schroeder TA, Komandur R, Schroeder TA. On Shear Instability in Machining a Nickel-Iron Base Superalloy. J Eng Ind May 1986;vol. 108(2): 93–100.
11. Schmidt A. Heat in metal cutting. ASM International; 1949
12. Kumar LD, Ajay V. Modelling of temperature profile in metal cutting process. Int J Innov Res Dev 2012;vol. 8:216–27.
13. Ueda T, Al Huda M, Yamada K, Nakayama K, Kudo H. Temperature Measurement of CBN Tool in Turning of High Hardness Steel. CIRP Ann Jan. 1999;vol. 48(1): 63–6.
14. H. Çalışkan, C. Kurbanoğlu, P. Panjan, M. Čekada, D. Kramar (2013). Wear behavior and cutting performance of nanostructured hard coatings on cemented carbide cutting tools in hard milling. Tribology International, 62, 215–222.
15. Q. An, C. Wang, J. Xu, P. Liu, M. Chen (2014). Experimental investigation on hard milling of high strength steel using PVD-AlTiN coated cemented carbide tool. International Journal of Refractory Metals and Hard Materials, 43, 94–101.
16. Q. Zhang, S. Zhang, J. Li (2017). Three Dimensional Finite Element Simulation of Cutting

Forces and Cutting Temperature in Hard Milling of AISI H13 Steel. Procedia Manufacturing, 10, 37–47.

17. B. Li, S. Zhang, Q. Zhang, J. Chen, J. Zhang (2019). Modelling of phase transformations induced by thermo-mechanical loads considering stress-strain effects in hard milling of AISI H13 steel. International Journal of Mechanical Sciences, 149, 241–253.
18. Devillez, A., Le Coz, G., Dominiak, S., & Dudzinski, D. (2011) Dry machining of Inconel 718: workpiece surface integrity. Journal of Materials Processing Technology, 211(8), 1590–1598.
19. Al-Falahi, M., Fadaeifard, F., Al-Falahi, M. D. A., Bin Baharudin, B. T. H. T., & Hong, T. S. (2016). *Surface damages and tool wear mode in end milling of Hastelloy-C276 under dry and wet conditions*. *Materialwissenschaft und Werkstofftechnik*, 47(12), 1182–1192.
20. Yıldırım, Ç. V., et al. (2023). *Analysis of machinability and sustainability aspects while machining Hastelloy C4 under sustainable cutting conditions*. *Sustainable Materials and Technologies*. doi:10.1016/j.susmat.2023.e00781
21. Arunachalam, R. M., Mannan, M. A.; "Machinability of Nickel-Based High Temperature Alloys"; *Machining Science and Technology*, 2000.
22. Ezugwu, E. O.; "Key Improvements in the Machining of Difficult-to-Cut Aerospace Superalloys"; *International Journal of Machine Tools and Manufacture*, 2005.
23. Thakur, A., Gangopadhyay, S.; "State-of-the-Art in Surface Integrity in Machining of Nickel-Based Super Alloys"; *International Journal of Machine Tools and Manufacture*, 2017.
24. Pawade, R. S., Joshi, S. S., Brahmankar, P. K.; "Effect of Machining Parameters on Surface Integrity in High-Speed Machining of Nickel-Based Superalloys"; *International Journal of Machine Tools and Manufacture*, 2007.